JACC: CARDIOVASCULAR IMAGING
VOL. 3, NO. 4, 2010

ISSN 1936-878X/10/$36.00
PUBLISHED BY ELSEVIER INC.
DOI:10.1016/j.jcmg.2010.01.004

CVN Interview

Feasibility of FDG Imaging of the Coronary Arteries

Comparison Between Acute Coronary Syndrome and Stable Angina

Ian S. Rogers, MD, MPH, Khurram Nasir, MD, MPH, Amparo L. Figueroa, MD, Ricardo C. Cury, MD, Udo Hoffmann, MD, MPH, David A. Vermylen, BS, Thomas J. Brady, MD, Ahmed Tawakol, MD

Boston, Massachusetts

OBJECTIVES This study tested the hypothesis that fluorodeoxyglucose (FDG) uptake within the ascending aorta and left main coronary artery (LM), measured using positron emission tomography (PET), is greater in patients with recent acute coronary syndrome (ACS) than in patients with stable angina.

BACKGROUND Inflammation is known to play an important role in atherosclerosis. Positron emission tomography imaging with ^{18}F-FDG provides a measure of plaque inflammation.

METHODS Twenty-five patients (mean age 57.9 ± 9.8 years, 72% male, 10 ACS, and 15 stable angina) underwent cardiac computed tomographic angiography and PET imaging with ^{18}F-FDG after invasive angiography. Images were coregistered, and FDG uptake was measured at locations of interest for calculation of target-to-background ratios (TBR). Additionally, FDG uptake was measured at the site of the lesion deemed clinically responsible for the presenting syndrome (culprit) by virtue of locating the stent deployed to treat the syndrome.

RESULTS The FDG uptake was higher in the ACS versus the stable angina groups in the ascending aorta (median [interquartile ranges] TBR 3.30 [2.69 to 4.12] vs. 2.43 [2.00 to 2.86], $p = 0.02$), as well as the LM (2.48 [2.30 to 2.93] vs. 2.00 [1.71 to 2.44], $p = 0.03$, respectively). The TBR was greater for culprit lesions associated with ACS than for lesions stented for stable coronary syndromes (2.61 vs. 1.74, $p = 0.02$). Furthermore, the TBR in the stented lesions (in ACS and stable angina groups) correlated with C-reactive protein ($r = 0.58$, $p = 0.04$).

CONCLUSIONS This study shows that in patients with recent ACS, FDG accumulation is increased both within the culprit lesion as well as in the ascending aorta and LM. This observation suggests inflammatory activity within atherosclerotic plaques in acute coronary syndromes and supports intensification of efforts to refine PET methods for molecular imaging of coronary plaques. (J Am Coll Cardiol Img 2010;3:388–97) © 2010 by the American College of Cardiology Foundation

From the Cardiac MR PET CT Program, Division of Cardiology and Department of Radiology, Massachusetts General Hospital, Harvard Medical School, Boston, Massachusetts. Drs. Rogers and Nasir received support from National Institutes of Health grant T32HL076136. Dr. Tawakol received support from the Center for Integration of Medicine and Innovative Technologies.

Manuscript received September 8, 2009; revised manuscript received January 20, 2010, accepted January 22, 2010.

The majority of myocardial infarctions (MI) and sudden cardiac deaths result from the rupture of plaques that in most cases did not cause significant flow limitations before the acute event (1,2). Although stenosis severity has proven a poor predictor of plaque rupture (3), several other plaque characteristics, notably plaque inflammation, have been strongly associated with plaque rupture and thrombosis (4–7). Imaging with fluorodeoxyglucose (FDG) positron emission tomography (PET) provides a reproducible measure of glycolysis (8), which has proven invaluable for the identification of small, metabolically active tissues such as tumors and inflamed lesions (9). Furthermore, FDG accumulation has been shown to provide an index of atherosclerotic inflammation, as demonstrated in animal models and humans (10–12). Several studies have shown that FDG activity within plaques correlates with inflammation in atherosclerosis (13–15). Furthermore, the vascular PET signal is reproducible (16,17) and is modifiable by interventions that have an anti-inflammatory effect (18).

Prior investigators have reported FDG accumulation in association with coronary vessels (19–22). However, the lack of a standard for coronary inflammation within those studies provided little evidence that the FDG uptake was related to plaque activity. Several factors impart formidable obstacles to coronary FDG PET imaging, including uptake of FDG by adjacent myocardium, the limited spatial resolution of PET, and the substantial motion of the coronary arteries. In the present study, we attempted to determine whether FDG uptake can be measured in the ascending aorta and in the relatively immobile left main coronary artery (LM) despite the known obstacles and whether the signal is increased in patients presenting with acute coronary syndrome (ACS). Moreover, we sought to test the hypothesis that FDG uptake is greatest within lesions that are expected to be inflamed: those plaques that are deemed to have recently caused an ACS. We took advantage of concurrent computed tomographic (CT) angiography for delineation of coronary activity and to identify the plaques associated with stents that were deployed to treat ACS. We sought to test the hypothesis that FDG uptake within plaques locations deemed responsible for ACS is greater than in remotely stented plaques, which are presumably less inflamed. Additionally, to exclude FDG uptake secondary to lesion manipulation, we compared FDG uptake in plaques recently stented for ACS with plaques recently stented for stable coronary syndromes.

METHODS

Patients. The study was performed in 25 patients (average age 58 ± 10 years, 72% men), 10 of whom presented with ACS requiring stent placement (ACS, n = 10). Of the remaining 15 patients with stable angina (n = 15), 5 presented with stable angina requiring stent placement (n = 5) and 10 presented with atypical or typical chest pain for which a coronary angiographic evaluation was required in the clinical judgment of the referring physicians. All subject cases were adjudicated for study group classification after eligibility determination and receiving informed consent. Subjects were classified as having experienced ACS (i.e., ST-segment elevation MI [n = 1], non–ST-segment elevation MI [n = 4], or unstable angina [n = 5]) or as having experienced stable angina (n = 15) based on the nature and chronicity of their chest pain, medical history, and available diagnostics (such as electrocardiograms [ECGs] and biomarkers), according to the American College of Cardiology/American Heart Association guideline definitions (23), and as supported by findings on coronary arteriography.

Patients were not eligible if they had diabetes mellitus, an allergy to iodinated contrast, renal dysfunction, hemodynamic instability, substantial arrhythmias, or decompensated heart failure. The study protocol was approved by the human research committee at the Massachusetts General Hospital, and informed consent was obtained from each subject.

Patient preparation. After catheterization, subjects underwent cardiac CT angiography and cardiac FDG PET imaging. To minimize myocardial glucose uptake in order to better visualize coronary FDG uptake, we took advantage of the myocardium's preference for free fatty acid over glucose as an energy source. On the day before imaging, subjects were asked to adhere to a very-low-carbohydrate, high-fat diet and then to fast overnight (24), followed by the administration of a high-fat, low-carbohydrate beverage 45 min before FDG injection (approximately 150 ml Atkins Advantage Shake, Atkins Nutritionals, Ronkonkoma, New York).

PET imaging. The PET imaging was performed 3 h after administration of 13 mCi of ^{18}F-FDG. The choice of time interval was based on previous work

ABBREVIATIONS AND ACRONYMS

ACS = acute coronary syndrome
CT = computed tomography
ECG = electrocardiogram
FDG = fluorodeoxyglucose
IL = interleukin
IQR = interquartile range
LAD = left anterior descending coronary artery
LCx = left circumflex coronary artery
LM = left main coronary artery
MI = myocardial infarction
PET = positron emission tomography
RCA = right coronary artery
ROI = region of interest
SUV = standardized uptake value
TBR = target-to-background ratio

(16,25). Despite the widespread availability of PET CT systems, we used a dedicated PET system (Siemens ECAT Exact HR+, Knoxville, Tennessee) to avoid the potential misregistration that can occur when CT attenuation maps are used to correct the PET volume data. The system provides 63 planes, a 15.5-cm field of view, and a maximum 4.2-mm intrinsic resolution at the center of the field of view. Data were acquired in 2-dimensional mode over 25 min, with subjects in the supine position. Image data were attenuation-corrected using PET transmission data; reconstructed using a conventional, filtered back-projection algorithm; and corrected for nonuniformity of detector responses, dead time, random coincidences, and scattered radiation.

Cardiac CT imaging. The CT imaging was performed on the same day as PET acquisition (Siemens Sensation 64, Forchheim, Germany). Subjects were premedicated with intravenous metoprolol and sublingual nitroglycerin unless medically contraindicated. Imaging was performed during an inspiratory breath hold, and ECG-triggered tube current modulation was used to reduce radiation exposure. Parameters included a slice collimation of 64×0.6 mm, temporal resolution of 165 ms, tube voltage of 120 kVp, and tube current of 850 mAs. Images were retrospectively gated to the ECG and reconstructed at 65% of the R-R interval using a medium-smooth kernel and slice thickness/increment of 0.75/0.4 mm.

Measurement of FDG uptake. The PET images were manually coregistered with CT images (Leonardo TrueD, Siemens Forchheim, Germany) by an investigator who was blinded to the patients' clinical history and classification. Perfect coregistration of chest structures between the PET and CT images was not feasible given the differences in cardiovascular and respirophasic motion affecting the major structures within the PET images (which were acquired over 25 min of free breathing) and the CT (which was ECG gated and acquired during a breath hold). Accordingly, we used a strategy of prioritizing the registration of the ascending aorta given that it is discernable on both PET and CT image sets and that its proximity to the tethered LM increases the likelihood of excellent LM coregistration in turn.

Once coregistered, the maximum standardized uptake value (SUV) of FDG was measured within the ascending aorta and within several pre-defined coronary locations. To accomplish this, CT images were used to guide placement of 5-mm^2 regions of interest (ROIs) over the vascular segment being measured and the maximum SUV value within each ROI was recorded. First, measurement of aortic activity was acquired as the average of 6 ROIs placed along the wall of the ascending aorta 20 mm above the aortic annulus. Next, SUV measurements were obtained in several pre-defined coronary locations in all subjects: the LM, the proximal and mid–left anterior descending (LAD), the left circumflex artery (LCx), and the right coronary artery (RCA). Activity in the LM was measured approximately 8 mm from the LM ostium to avoid spillover of activity from the aorta. Activity in the proximal and mid-LAD and LCx was measured approximately 8 and 16 mm from the bifurcation or trifurcation, and activity in the proximal and mid-RCA was measured approximately 8 and 16 mm from the RCA ostium. Next, FDG uptake was measured at the site of the culprit coronary lesion, which was defined as the coronary segment deemed by the clinical team to be responsible for the syndrome, for which a stent was deployed at presentation. The culprit lesion was in turn identified on the CT images by locating the stent. The ROI was placed at the location of highest plaque activity overlying the stent, and the maximum SUV was recorded.

To obtain a background value for FDG uptake, blood SUV was determined by placement of 6 1-cm^3 ROIs within the left atrial cavity in locations devoid of significant spillover activity. The mean SUV value for each ROI was measured and the average of the 6 arterial values was recorded. Afterward, a target-to-background ratio (TBR) was calculated for each vascular segment measured as the segment maximum SUV divided by atrial blood mean SUV.

Suppression of myocardial FDG uptake was assessed according to the qualitative visual grading scale proposed by Williams and Kolodny (24): 0 = minimal uptake; 1 = mostly minimal or mild uptake; 2 = mostly intense or moderate uptake; 3 = homogeneously intense.

To evaluate interobserver reliability of the coregistration and measurement process, images from 10 randomly selected patients were independently coregistered by 2 investigators (A.T., I.R.) on 2 separate occasions. The investigators were blinded to all information regarding the case, including clinical history and group classification of each subject. Aortic and coronary measurements were repeated as previously described.

Blood biomarkers. Blood was collected from subjects on the day of imaging before FDG injection or

image acquisition. Several inflammatory biomarkers were measured, including high-sensitivity C-reactive protein (CRP), CD40, intercellular adhesion molecule-1, interleukin-12 p70 (IL-12 p70), tumor necrosis factor-alpha, immunoglobulin M, and vascular cell adhesion molecule-1, via multiplexed immunoassay (Rules-Based Medicine, Inc., Austin, Texas).

Statistical methods. Analysis of the baseline characteristics of the ACS and stable groups was conducted through the use of *t* tests for normal continuous variables, Wilcoxon rank sum tests for nonnormal continuous variables, and Fisher exact tests for binary variables. The TBR data are presented as median and interquartile range (IQR), and the differences between the groups were assessed by Wilcoxon rank sum tests. Correlations are reported as Spearman correlation coefficients. Intraclass correlation coefficients were calculated to determine interobserver reliability using the mean SUV values obtained by the readers during the reliability analysis. All analyses were performed with SAS (version 9.1, SAS Institute, Inc., Cary, North Carolina). A value of $p < 0.05$ was considered significant.

RESULTS

Demographic information regarding the enrolled patients are summarized in Table 1. The PET/CT examination was performed within a median of 8 days (IQR 3 to 21 days) in patients with recent stent placement for ACS and within a median of 16 days (IQR 8 to 22 days) in patients with recent stent placement for stable angina. The difference in time from stent placement between groups was not significant ($p = 0.62$).

Myocardial FDG suppression and image quality. Myocardial uptake of FDG was minimal in 10 of 25 (40%) subjects, mostly minimal or mild in 11 of 25 (44%) subjects, mostly intense or moderate in 3 of 25 (12%) subjects, and homogeneously intense in 1 (4%) subject. There was no difference in the degree of myocardial uptake among subject groups ($p = 0.93$). In the 25 patients studied, 100% (25) of ascending aortas and left main segments were evaluable. A total of 175 total coronary segments were investigated, 96% (168 of 175) of which were evaluable by PET. Seven segments (4%) could not be evaluated because of spillover of adjacent myocardial uptake. The blinded interobserver reliability analysis for the coregistration process revealed intraclass correlation coefficients between readers of 0.92 in the ascending aorta, 0.97 in the LM, 0.84 in the proximal LAD, 0.99 in the proximal LCx, and 0.29 in the proximal RCA.

Vascular FDG accumulation. CULPRIT LESION ACTIVITY. Analysis of the PET signal within stented lesions was feasible in 89% (24 of 27) of all stented lesions, including 8 of 10 in the ACS group and 16 of 17 in the stable angina group (Table 2). The PET signal (given as median TBR [IQR]) within the culprit

Table 1. Baseline Characteristics of the Subjects

	ACS Group (n = 10)	Stable Group (n = 15)	p Value*
Age (yrs)	55.7 ± 10.1	58.5 ± 10.1	0.50
Male sex (%)	70	73.3	1.00
History of CAD (%)	20	66.7	0.04
Family history of CV disease <60 yrs (%)	10	46.7	0.09
Total cholesterol (mg/dl)	186 ± 40.6	172 ± 36.7	0.37
HDL cholesterol (mg/dl)	47.1 ± 13.7	44 ± 10.7	0.53
LDL cholesterol (mg/dl)	102.7 ± 32.2	100.4 ± 31.5	0.86
Triglycerides (mg/dl)	171 ± 90.5	154.8 ± 102.6	0.62
Statin use (%)	70	73.3	1.00
Systolic blood pressure (mm Hg)	125.8 ± 19.4	128.13 ± 17.5	0.76
Hypertension (%)	80	93.3	0.54
Antihypertensive therapy (%)	80	93.3	0.54
Current smoking (%)	50	20	0.19
Body mass index (kg/m^2)	27.4 ± 3.5	30.9 ± 4.2	0.04
Framingham risk score	10.3 ± 8.4	6.5 ± 6.8	0.23

Continuous values are presented as mean ± SD. Binary values are presented as percentages. *p values for statistical difference between groups are calculated by 2-sample Student *t* tests (continuous values) and Fisher exact tests (binary values).
ACS = acute coronary syndrome; CAD = coronary artery disease; CV = cardiovascular; HDL = high-density lipoprotein; LDL = low-density lipoprotein.

Table 2. Summary of Subject Presentation and TBR Measurements

Age (yrs)	Sex	Clinical Presentation	TBR						
			Ascending Aorta	Left Main	Proximal LAD	Proximal LCx	Proximal RCA	Recent Stent	Remote Stent
			ACS						
38	F	UAP: accelerating CP with anterior T-wave inversions	++++	++	++++	++++	++	++++	
60	M	NSTEMI: accelerating angina, CP at rest	++++	++++	+++	+++	++	+++	
43	M	UAP: CP at rest with ECG changes	++++	++	++	+	++	*	
51	F	NSTEMI: acute-onset CP at rest	+++	++	++	+	++	++	
65	M	UAP: CP radiating to left arm with ST-segment depressions	+++	++	+	+	+	++	
53	M	UAP: new-onset exertional CP with minimal exertion	++	++	*	+	++	+++	
59	F	STEMI: acute tent thrombosis 1 week after BMS placement.	++	++	*	++	+	++	
62	M	UAP: acute-onset CP with minimal exertion	++	++	*	++	+	++	
69	M	NSTEMI: acute-onset CP at rest	++	++	++	++	+	++	
63	M	NSTEMI: acute-onset CP at rest	+++	+++	+++	++	++	*	
			Stable angina requiring PCI						
43	M	CP syndrome over several months	+	+	+	+	+	+	
55	M	CP syndrome over several months	++	++	+	+	+	+	—
50	F	CP syndrome over several months	++	++	+	+	+	*	+
65	M	CP syndrome over several months	+++	++	++	+	++	++	+
78	M	CP syndrome over several months	++	+	+	+	+	+	
			Stable angina not requiring PCI						
55	F	Cardiomyopathy, no significant stenosis	+	+	+	+	−		
56	M	Stable CP: medical management of CAD	++++	+++	++	++	+		+
58	F	Stable CP: medical management of CAD	++	++	++	++	+		
74	F	Remote MI, new CP; no new stenosis	++	+	+	+	+		+
57	M	Stable CP: medical management of CAD	++	++	++	++	+		
46	M	Recent-onset CP; mild CAD on catheterization	+++	++	++	++	+		
64	M	Stable CP: medical management of CAD	+	++	+	++	+		++
50	M	Stable CP: medical management of CAD	++	++	+	+	+		+
66	M	Stable CP: medical management of CAD	++	++	+	++	+		
67	M	Stable CP: medical management of CAD	++	++	++	++	+		++

− = TBR <1; + = TBR 1.00 to 1.99; ++ = TBR 2.0 to 2.99; +++ = TBR 3.0 to 3.99; ++++ = TBR of 4.0 or greater. *Segment excluded due to spillover or location.

CP = chest pain; ECG = electrocardiogram; LAD = left anterior descending coronary artery; LCx = left circumflex coronary artery; MI = myocardial infarction; NSTEMI = non–ST-segment elevation myocardial infarction; PCI = percutaneous coronary infusion; RCA = right coronary artery; STEMI = ST-segment elevation myocardial infarction; TBR = target-to-background ratio; UAP = unstable angina pectoris; other abbreviations as in Table 1.

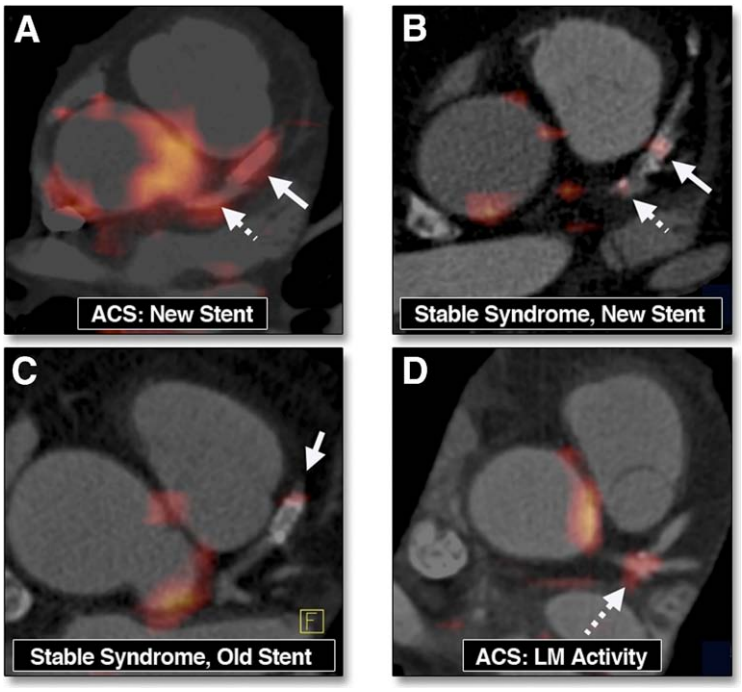

Figure 1. Coregistered FDG PET/CT Images Show FDG Uptake Within Specified Coronary Vascular Locations

Arrows show stent locations. **Hatched arrows** show lesions within the LM. **(A)** Increased uptake in both LM and stented culprit lesions in a subject presenting with ACS. **(B)** More modest uptake in a coronary lesion that was recently stented for a stable coronary syndrome (some FDG uptake is also noted in a mixed plaque within the LM). **(C)** Modest FDG uptake within a lesion stented several months before imaging. **(D)** The FDG uptake at the trifurcation of the LM in a subject presenting with ACS. ACS = acute coronary syndrome; CT = computed tomography; FDG = fluorodeoxyglucose; LM = left main coronary artery; PET = positron emission tomography.

lesions in patients with ACS (2.61 [2.27 to 3.45]) was higher than in stable angina patients (1.74 [1.14 to 2.0], p = 0.02) (Figs. 1 and 2). In contrast, there was no significant difference in plaque activity between newly stented stable angina plaques and remotely stented plaques (p = 0.49). Additionally, plaque TBR was significantly higher within the culprit lesions of patients presenting with ACS than within the proximal vessels of these same patients (2.61 [2.27 to 3.45] vs. 1.88 [1.3 to 2.4], p = 0.04).

Of the 8 culprit lesions evaluated in ACS, 5 received bare-metal stents and 3 received drug-eluting stents. Of the 16 stented segments in the stable angina group, 6 received bare-metal stents and 10 received drug-eluting stents. There was no difference in TBR between plaques stented with bare-metal stents versus drug-eluting stents in the ACS group (p = 0.70) or among all subjects (p = 0.55). Similarly, there was no correlation between TBR and: 1) stent diameter in either the ACS group (Spearman r = 0.08, p = 0.86) or among all subjects (r = −0.02, p = 0.95); or 2) stent length in either the ACS group (r = 0.39, p = 0.39) or among all subjects (r = −0.31, p = 0.17).

Other vascular activity. The PET signal within the ascending aorta was higher in subjects presenting with ACS versus stable angina (values given as median TBR [IQR]) (3.30 [2.73 to 4.0] vs. 2.43 [2.00 to 2.9], p = 0.02). Examples of a subject with increased FDG uptake in the ascending aorta are shown in Figure 3. Similarly, the PET signal was significantly greater within the LM of subjects presenting with ACS versus stable angina (2.48 [2.30 to 2.93] vs. 2.00 [1.71 to 2.44], p = 0.03) (Fig. 4). Although the signal within the proximal and mid-LAD segments was higher in ACS versus stable groups (2.20 vs. 1.75 and 1.50 vs. 1.0, p = 0.03 and p = 0.04, respectively), the signals in the proximal LCx and proximal RCA were not significantly different between the 2 groups (2.00 vs. 1.75 and 2.17 vs. 1.60, for median TBR in ACS vs. stable angina in LCx and RCA, p = 0.30 and p = 0.059, respectively).

Blood biomarkers. Subjects with ACS had a higher blood level of log high-sensitivity CRP and IL-12 p70 than stable angina subjects (p = 0.02 and p = 0.02, respectively). Moreover, several blood inflammatory biomarkers correlated with the activity mea-

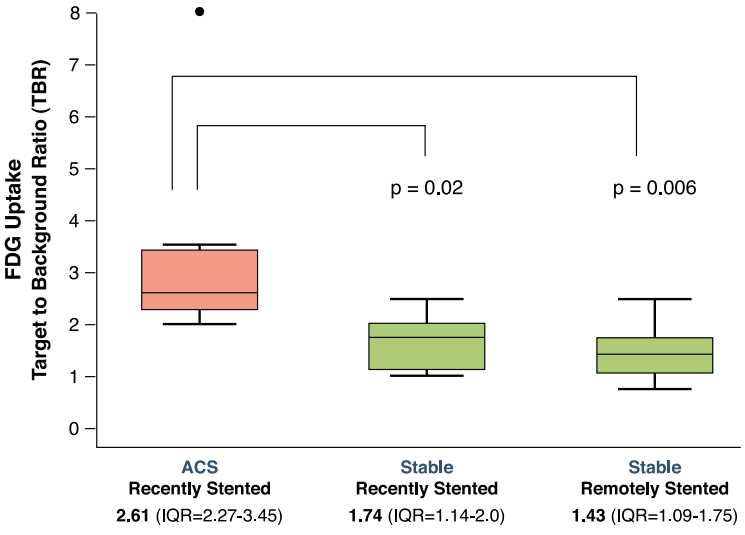

Figure 2. Box Plot Comparison of Interquartile Ranges of TBRs of Stented Plaques Among Study Groups

The median TBR within the culprit lesions of subjects with ACS (2.61) was significantly higher (p = 0.02) than the median TBR within culprit lesions in stable angina subjects (1.74) and significantly higher (p = 0.006) than within previously stented plaques in stable angina subjects (1.43). There was no significant difference in median TBR between culprit lesions in stable angina patients and remotely stented plaques (p = 0.49). ACS = acute coronary syndrome; TBR = target-to-background ratio.

sured within stented segments. The TBR in the plaques treated for ACS or stable angina correlated with levels of CRP (r = 0.58, p = 0.04), immunoglobulin M (r = 0.77, p = 0.002), IL-12 p70 (r = 0.62, p = 0.02), and tumor necrosis factor-α (r = 0.56, p = 0.048).

DISCUSSION

Within this feasibility study, we found for the first time that FDG uptake in the ascending aorta and LM is increased in patients with ACS compared with patients with stable angina. Furthermore, we found that FDG uptake is greater in lesions judged to be responsible for ACS compared with lesions associated with stable coronary syndromes.

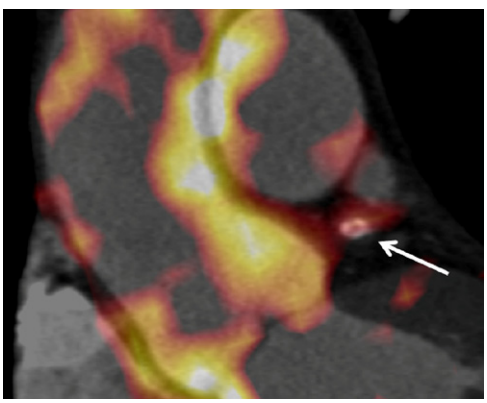

Figure 3. FDG Uptake in ACS

Coregistered FDG PET/CT images show increased FDG uptake in the ascending aorta and in a culprit plaque in the LAD **(arrow)** in a 60-year-old man who presented with ACS. LAD = left anterior descending coronary artery; other abbreviations as in Figure 1.

The correlation of ^{18}F-FDG uptake and atherosclerotic inflammation has been previously demonstrated in animal and human studies. Studies in humans show that FDG uptake correlates strongly with plaque inflammation (20) and that the measurement of atherosclerotic FDG signal is highly reproducible with intraclass correlation coefficients between 0.90 and 0.98 in medium to large arteries (16). Furthermore, the plaque signal is modifiable, as demonstrated in animal models and clinical trials (18,26–28). Consistent with the concept that ACS is associated with an enhanced inflammatory milieu, we found that FDG uptake in the ascending aorta was greater in patients presenting with ACS than in stable angina patients. Similarly, we observed an increase in the PET signal within the LM of patients presenting with ACS.

One important prior obstacle to demonstrating feasibility coronary plaque imaging with PET had been the lack of a standard to support the contention that the observed hot spots were indeed derived from coronary plaques. In this study, we developed a reference point for clinically significant (culprit) lesions with a position that is conveniently marked by a stent placed at the location deemed to be the

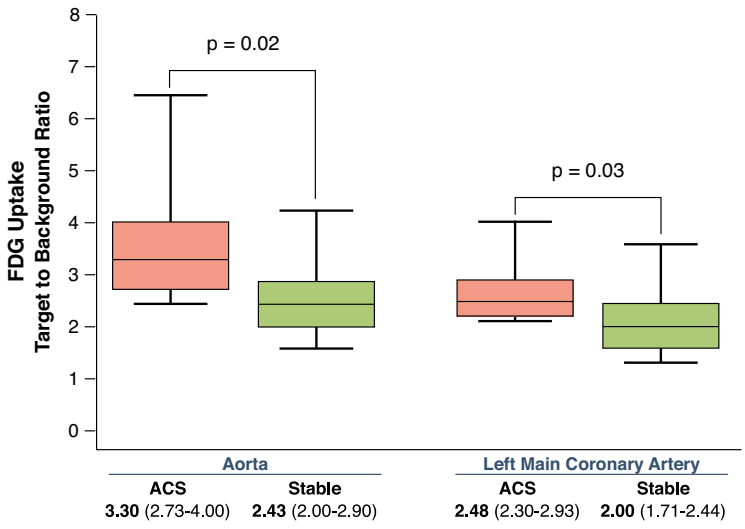

Figure 4. Box Plot Comparison of Interquartile Ranges of TBRs Within the Ascending Aorta and LM Between Study Groups

The median TBR within the ascending aorta of subjects with ACS (3.30) was significantly higher ($p = 0.02$) than the median TBR in stable angina subjects (2.43). The median TBR within the LM of subjects with ACS (2.48) was significantly higher ($p = 0.03$) than the median TBR in stable angina subjects (2.00). **Horizontal lines** are medians, **ends of boxes** are upper and lower quartiles, and **vertical lines** are full range of data values. LM = left main coronary artery; other abbreviations as in Figure 2.

culprit lesion at the time of catheterization. We found that FDG uptake within culprit lesions ACS, which as a group are known to substantially inflamed (29), was significantly higher than within stable angina plaques. Furthermore, a significant difference remained when activity within recently stented stable angina plaques and remotely stable angina plaques were compared, suggesting that the increased signal observed in ACS was related to the underlying inflammation and not solely a consequence of vascular injury after stent placement.

To minimize the impact of coronary motion on our image analysis, we prioritized the coregistration of the ascending aorta, which conveniently tends to show increased FDG uptake (16,30) in patients with atherosclerosis. Coregistration of the ascending aorta in turn yielded excellent registration of the proximal coronary tree. Additionally, we directed our attention to the LM, which is tethered to the aorta and has a nonepicardial location, thus it experiences less motion within the cardiac cycle (31) and is less susceptible to interference by myocardial FDG uptake. Even in cases of excellent myocardial suppression of FDG activity, enough residual activity remained to permit registration of the cardiac structures. It should be noted that ECG gating of the PET acquisition was initially attempted in the development of this protocol but was not ultimately used because in our experience the loss of PET data associated with gating offset its advantage of reduced motion. However, we believe that refinements in gating methods, such as those reported by Suzuki et al. (32), might prove useful for coronary PET imaging.

Study limitations. We observed that the coregistration and measurement process was highly reproducible within the ascending aorta, LM, proximal LAD, and proximal LCx, whereas measurements in the RCA and in the mid- and distal coronary tree were substantially less reproducible. We posit that the limited reproducibility in the RCA and the distal coronary tree likely relates to the well-described relative increase in coronary motion in those locations. Although efficiency in the coregistration of images improved significantly with experience, the process remains time consuming and will require continued development before implementation outside of a research setting.

It is important to note that the inflammatory signal measured in our patients with ACS might not reflect the state of the signal just before the clinical presentation. Either the systemic inflammatory milieu associated with the acute ACS, the additional inflammation associated with stenting, or both might have contributed to the high PET signals that we measured in our patients with ACS after their stent implantations. It is possible that if the ACS subjects were hypothetically imaged just before their events, the measurable vascular PET signal might not have been different from that of

stable subjects. Ongoing studies examining the impact of therapies on the coronary PET signals should yield further insights. Moreover, natural history studies will be needed to evaluate whether the aortic and coronary PET signals have clinical utility.

CONCLUSIONS

The findings of this study show the feasibility of FDG imaging of the LM and that vascular activity is increased in the aorta and LM of patients presenting with ACS. Furthermore, we observed increased FDG uptake associated with culprit coronary lesions in patients presenting with ACS. Because FDG uptake serves as an index of plaque inflammation, this imaging approach may provide insights regarding the state of inflammation within the coronary vasculature. These observations support further efforts to refine PET methods to image coronary plaque inflammation.

Reprint requests and correspondence: Dr. Ahmed Tawakol, Cardiac MR PET CT Program, Massachusetts General Hospital, 165 Cambridge Street, Suite 400, Boston, Massachusetts 02114-2750. *E-mail: atawakol@partners.org.*

REFERENCES

1. Virmani R, Kolodgie FD, Burke AP, Farb A, Schwartz SM. Lessons from sudden coronary death: a comprehensive morphological classification scheme for atherosclerotic lesions. Arterioscler Thromb Vasc Biol May 2000;20:1262–75.
2. Ambrose JA, Tannenbaum MA, Alexopoulos D, et al. Angiographic progression of coronary artery disease and the development of myocardial infarction. J Am Coll Cardiol 1988; 12:56–62.
3. Falk E, Shah PK, Fuster V. Coronary plaque disruption. Circulation 1995; 92:657–71.
4. Fuster V, Lewis A. Conner Memorial Lecture. Mechanisms leading to myocardial infarction: insights from studies of vascular biology (erratum Circulation 1995;91:256). Circulation 1994;90:2126–46.
5. Muller JE, Abela GS, Nesto RW, Tofler GH. Triggers, acute risk factors and vulnerable plaques: the lexicon of a new frontier. J Am Coll Cardiol 1994;23:809–13.
6. Burke AP, Farb A, Malcom GT, Liang YH, Smialek J, Virmani R. Coronary risk factors and plaque morphology in men with coronary disease who died suddenly. N Engl J Med 1997;336:127.
7. Farb A, Burke AP, Tang AL, et al. Coronary plaque erosion without rupture into a lipid core. A frequent cause of coronary thrombosis in sudden coronary death. Circulation 1996;93: 1354–63.
8. Silverman DH, Hoh CK, Seltzer MA, et al. Evaluating tumor biology and oncological disease with positron-emission tomography. Semin Radiat Oncol 1998;8:183–96.
9. Phelps M. Positron emission tomography provides molecular imaging of biological processes. Proc Natl Acad Sci U S A 2000;97:9226–33.
10. Hara M, Goodman PC, Leder RA. FDG-PET finding in early-phase Takayasu arteritis. J Comput Assist Tomogr 1999;23:16–8.
11. Meller J, Altenvoerde G, Munzel U, et al. Fever of unknown origin: prospective comparison of [18F]FDG imaging with a double-head coincidence camera and gallium-67 citrate SPET. Eur J Nucl Med 2000;27: 1617–25.
12. Blockmans D, Maes A, Stroobants S, et al. New arguments for a vasculitic nature of polymyalgia rheumatica using positron emission tomography. Rheumatology 1999;38:444–7.
13. Derdelinckx I, Maes A, Bogaert J, Mortelmans L, Blockmans D. Positron emission tomography scan in the diagnosis and follow-up of aortitis of the thoracic aorta. Acta Cardiol 2000;55:193–5.
14. Lederman RJ, Raylman RR, Fisher SJ, et al. Detection of atherosclerosis using a novel positron-sensitive probe and 18-fluorodeoxyglucose (FDG). Nucl Med Commun 2001;22:747–53.
15. Rudd JH, Warburton EA, Fryer TD, et al. Imaging atherosclerotic plaque inflammation with [18F]-fluorodeoxyglucose positron emission tomography. Circulation 2002;105:2708–11.
16. Rudd JH, Myers KS, Bansilal S, et al. (18)Fluorodeoxyglucose positron emission tomography imaging of atherosclerotic plaque inflammation is highly reproducible: implications for atherosclerosis therapy trials. J Am Coll Cardiol 2007;50:892–6.
17. Rudd JH, Myers KS, Bansilal S, et al. Atherosclerosis inflammation imaging with 18F-FDG PET: carotid, iliac, and femoral uptake reproducibility, quantification methods, and recommendations. J Nucl Med 2008;49:871–8.
18. Tahara N, Kai H, Ishibashi M, et al. Simvastatin attenuates plaque inflammation: evaluation by fluorodeoxyglucose positron emission tomography. J Am Coll Cardiol 2006;48:1825–31.
19. Alexanderson E, Slomka P, Cheng V, et al. Fusion of positron emission tomography and coronary computed tomographic angiography identifies fluorine 18 fluorodeoxyglucose uptake in the left main coronary artery soft plaque. J Nucl Cardiol 2008;15:841–3.
20. Dunphy MP, Freiman A, Larson SM, Strauss HW. Association of vascular 18F-FDG uptake with vascular calcification. J Nucl Med 2005;46:1278–84.
21. Wykrzykowska J, Lehman S, Williams G, et al. Imaging of inflamed and vulnerable plaque in coronary arteries with 18F-FDG PET/CT in patients with suppression of myocardial uptake using a low-carbohydrate, high-fat preparation. J Nucl Med 2009;50:563–8.
22. Alexanderson E, Slomka P, Cheng V, et al. Fusion of positron emission tomography and coronary computed tomographic angiography identifies fluorine 18 fluorodeoxyglucose uptake in the left main coronary artery soft plaque. J Nucl Cardiol 2008;15:841–3.
23. Anderson JL, Adams CD, Antman EM, et al. ACC/AHA 2007 guidelines for the management of patients with unstable angina/non–ST-elevation myocardial infarction. J Am Coll Cardiol 2007;50:e1–e157.
24. Williams G, Kolodny G. Suppression of myocardial 18F-FDG uptake by preparing patients with a high-fat, low-carbohydrate diet. AJR Am J Roentgenol 2008;190:W151–6.
25. Tawakol A, Migrino RQ, Bashian GG, et al. In vivo 18F-fluorodeoxyglucose positron emission tomography imaging provides a noninvasive measure of carotid plaque inflammation in patients. J Am Coll Cardiol 2006;48:1818–24.

26. Ogawa M, Magata Y, Kato T, et al. Application of 18F-FDG PET for monitoring the therapeutic effect of antiinflammatory drugs on stabilization of vulnerable atherosclerotic plaques. J Nucl Med 2006;47:1845–50.
27. Worthley SG, Zhang ZY, Machac J, et al. In vivo non-invasive serial monitoring of FDG-PET progression and regression in a rabbit model of atherosclerosis. Int J Cardiovasc Imag 2009; 25:251–7.
28. Zhao Y, Kuge Y, Zhao S, Strauss HW, Blankenberg FG, Tamaki N. Prolonged high-fat feeding enhances aortic 18F-FDG and 99mTc-annexin A5 uptake in apolipoprotein E-deficient and wild-type C57BL/6J mice. J Nucl Med 2008;49:1707–14.
29. Fuster V, Moreno PR, Fayad ZA, Corti R, Badimon JJ. Atherothrombosis and high-risk plaque: part I: evolving concepts. J Am Coll Cardiol 2005;46:937–54.
30. Bural GG, Torigian DA, Chamroonrat W, et al. FDG-PET is an effective imaging modality to detect and quantify age-related atherosclerosis in large arteries. Nucl Med Biol 2006;33: 1037–43.
31. Achenbach S, Ropers D, Holle J, Muschiol G, Daniel WG, Moshage W. In-plane coronary arterial motion velocity: measurement with electron- beam CT. Radiology 2000;216:457–63.
32. Suzuki Y, Slomka PJ, Wolak A, et al. Motion-frozen myocardial perfusion SPECT improves detection of coronary artery disease in obese patients. J Nucl Med 2008;49:1075–9.

Key Words: 18-fluorodeoxyglucose positron emission tomography ■ cardiac computed tomography ■ aorta ■ coronary arteries ■ inflammation.

▶APPENDIX

For Online Figure 1, please see the online version of this article.